

# GPTrace: Effective Crash Deduplication Using LLM Embeddings

Patrick Herter

Fraunhofer AISEC

Garching near Munich, Germany

Technical University of Munich

Munich, Germany

patrick.herter@aisec.fraunhofer.de

Ridvan Açılan

Technical University of Munich

Munich, Germany

ridvan-acilan@hotmail.de

Vincent Ahlrichs

Fraunhofer AISEC

Garching near Munich, Germany

Technical University of Munich

Munich, Germany

vincent.ahlrichs@aisec.fraunhofer.de

Julian Horsch

Fraunhofer AISEC

Garching near Munich, Germany

julian.horsch@aisec.fraunhofer.de

## Abstract

Fuzzing is a highly effective method for uncovering software vulnerabilities, but analyzing the resulting data typically requires substantial manual effort. This is amplified by the fact that fuzzing campaigns often find a large number of crashing inputs, many of which share the same underlying bug. Crash deduplication is the task of finding such duplicate crashing inputs and thereby reducing the data that needs to be examined. Many existing deduplication approaches rely on comparing stack traces or other information that is collected when a program crashes. Although various metrics for measuring the similarity of such pieces of information have been proposed, many do not yield satisfactory deduplication results. In this work, we present GPTrace, a deduplication workflow that leverages a large language model to evaluate the similarity of various data sources associated with crashes by computing embedding vectors and supplying those as input to a clustering algorithm. We evaluate our approach on over 300 000 crashing inputs belonging to 50 ground truth labels from 14 different targets. The deduplication results produced by GPTrace show a noticeable improvement over hand-crafted stack trace comparison methods and even more complex state-of-the-art approaches that are less flexible.

## CCS Concepts

• **Software and its engineering** → **Software testing and debugging**; • **Security and privacy** → *Software and application security*.

## Keywords

software security, fuzzing, deduplication, stack traces, large language models, embeddings

## ACM Reference Format:

Patrick Herter, Vincent Ahlrichs, Ridvan Açılan, and Julian Horsch. 2026. GPTrace: Effective Crash Deduplication Using LLM Embeddings. In *2026 IEEE/ACM 48th International Conference on Software Engineering (ICSE '26)*, April 12–18, 2026, Rio de Janeiro, Brazil. ACM, New York, NY, USA, 12 pages. <https://doi.org/10.1145/3744916.3773161>

ICSE '26, Rio de Janeiro, Brazil

© 2026 Copyright held by the owner/author(s).

This is the author's version of the work. It is posted here for your personal use. Not for redistribution. The definitive Version of Record was published in *2026 IEEE/ACM 48th International Conference on Software Engineering (ICSE '26)*, April 12–18, 2026, Rio de Janeiro, Brazil, <https://doi.org/10.1145/3744916.3773161>.

## 1 Introduction

Fuzzing is one of the most popular and effective methods for testing software and finding security vulnerabilities therein. A fuzzing tool generates a large amount of test inputs either by randomized mutation of a valid seed corpus or by deriving them from a specification format. Inputs that cause a crash of the target software are collected along with some related information about the crash. Using these *sample crashing inputs (SCIs)*, developers try to analyze their software's behavior, find the underlying bugs, and fix them. However, fuzzing campaigns tend to produce thousands of SCIs, among which many trigger the same underlying bug. This results in significant resources being spent on organizing, assigning, and analyzing issues, only to find that many are duplicates.

Deduplication tools aim to remedy this by attempting to group SCIs that likely trigger the same underlying bug. A common deduplication approach (employed, e.g., by Crashwalk [28], TraceSim [39] and ReBucket [6]) is to collect stack traces when the SCIs trigger a crash and define a suitable notion of similarity of these stack traces. Similarity scores can then be used to decide which SCIs should be grouped together. Many approaches that deduplicate based on stack trace analysis devise hand-crafted algorithms that produce similarity scores based on the syntactic properties of stack traces. These are often inflexible and fail to capture the full information that is contained in stack traces, thus yielding unsatisfactory results.

With the emergence of large language models (LLMs) we have a new tool at our disposal to process textual input in various ways. Internally, LLMs use vectors of numbers to represent input queries. These *embeddings* ought to capture the semantic meaning of the input such that distances between embedding vectors reflect the similarity of the corresponding inputs. Our proposed deduplication method, GPTrace, computes LLM embeddings of stack traces and AddressSanitizer (ASan) [10] reports. Using standard distance functions on numerical vectors, e.g., the Euclidean metric, we can run clustering algorithms, such as Hierarchical Density-Based Spatial Clustering of Applications with Noise (HDBSCAN) [3, 23, 24], on the embedding vectors and thereby obtain a grouping of our SCIs.

By leveraging LLM embeddings and the contained knowledge gained from large amounts of data that were used during training of the LLM, GPTrace can extract more information from the supplied stack traces and ASan reports, and provide more robust similarity assessments than existing fixed, hand-crafted stack trace analysis

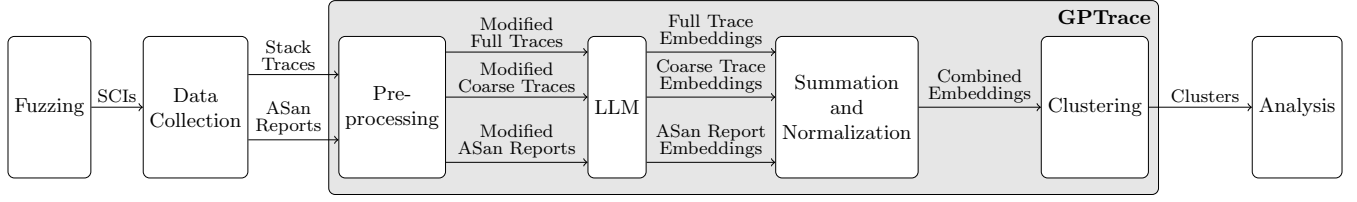


Figure 1: Overview of the GPTrace workflow.

methods. This manifests itself in accurate deduplication results that improve on those of existing stack trace deduplication approaches and even more sophisticated approaches that require more detailed execution information, such as Igor [15] or DeFault [42]. Moreover, GPTrace’s flexible design enables integration of different kinds of crash data on a per-target basis and can be adapted for use with targets written in different programming languages.

In summary, our concrete contributions are the following:

- A concept for leveraging LLM embeddings for the purpose of crash deduplication.
- A prototype implementation of GPTrace written in Python for deduplication of SCIs for C/C++ programs, which we provide as open source.<sup>1</sup>
- An extensive evaluation of different variants of GPTrace as well as comparisons to existing deduplication approaches. Our artifacts for the evaluation are also publicly available.<sup>1</sup>

In the rest of this paper, we present the design of GPTrace (Section 2) in detail and then discuss some notable points about our prototype implementation (Section 3). Next, we present the results of our evaluation (Section 4), including a comparison of GPTrace to previous crash deduplication methods. Finally, we talk about related work (Section 5) before drawing a conclusion (Section 6).

## 2 Design

In this section, we describe the design of GPTrace, an overview of which is shown in Figure 1. For each SCI returned by a fuzzing tool, GPTrace processes associated data that contains information about the crashing behavior of that SCI. Valuable information is carried by stack traces and ASan reports captured during the execution of the target software with the SCI. As a first step, these data sources undergo a preprocessing phase, during which several modifications take place. Next, GPTrace collects for each of these modified data sources the associated LLM embedding. We combine these individual embedding vectors for each SCI and then employ a clustering process that yields as a result our final bucketing of the SCIs.

### 2.1 Preprocessing

Before computing embeddings, GPTrace applies modifications to each of the input data sources. For every SCI, we use two versions of the same stack trace. We found that for some targets, stack traces can contain thousands of copies of the same frame. To reduce the size of the processed data, we keep only the topmost copy and discard all others from both versions of the stack trace. In addition to this, the second version of the stack trace is heavily shortened

by removing all function arguments from it. This results in stack traces that only contain coarse but crucial information, which is thereby given more weight in the following steps.

ASan reports also contain a copy of the stack trace. However, since GPTrace tracks this information separately, the traces are removed from the reports to give more weight to the crucial ASan information. A simpler approach would be to not process the stack traces separately and instead to solely rely on ASan reports with the contained stack traces. However, we show in Section 4.3 that processing these pieces of data separately improves the results.

To further increase the signal-to-noise ratio, we also remove the shadow byte map and legend that ASan reports contain. Examples of full and coarse stack traces as well as a modified ASan report produced this way are shown in Figure 2. Before moving on to the next step, GPTrace searches the processed data for duplicate entries for which all modified data sources are identical, and discards them.

### 2.2 Embedding

After preparing the various data sources, GPTrace uses an LLM to compute embeddings. These embeddings are vectors of numbers that are used by the LLM for its internal processing. As such, they capture the semantic meaning of the input from the point of view of the LLM. The distance between embedding vectors of different inputs determines how similar these inputs are in the perception of the LLM. This is the key principle that GPTrace leverages.

In more detail, GPTrace obtains a separate embedding vector  $v_{d,s}$  for each data source  $d \in D := \{\text{Full Traces, Coarse Traces, ASan Reports}\}$  and each  $s \in \{\text{SCIs}\}$ . We then combine, for a given  $s \in \{\text{SCIs}\}$ , the various  $v_{d,s}$ ,  $d \in D$ , into a single vector as follows:

$$v_s := \sum_{d \in D} \frac{v_{d,s}}{\|v_{d,s}\|}.$$

Here,  $\|\cdot\|$  denotes the Euclidean norm, and the normalization ensures that one vector does not dominate the others in the sum due to large entries. In practice, LLMs often produce embedding vectors that are already normalized. We decided to sum the vectors instead of concatenating them in order to enhance features that are shared across data sources: Each dimension of the resulting embedding vectors corresponds to some feature that the LLM associates with the input, independent of the data source. Summing the vectors amplifies a feature in the resulting vector if it is present in multiple data sources, while concatenating would keep them separate. Additionally, concatenation would produce higher-dimensional vectors, which tends to degrade the performance of clustering algorithms.

Quantifying the similarity of the obtained vectors during the clustering phase requires a distance function. While the cosine

<sup>1</sup> <https://github.com/Fraunhofer-AISEC/gptrace-artifacts>

```
#0 0xf7fc4579 in __kernel_vsyscall ()
#1 0xf7799eb7 in ?? () from /lib32/libc.so.6
#2 0xf77494c5 in raise () from /lib32/libc.so.6
#3 0xf77323ac in abort () from /lib32/libc.so.6
#4 0x0815f276 in __sanitizer::Abort() ()
#5 0x0815d377 in __sanitizer::Die() ()
#6 0x08138f8f in __asan::ReportGenericError(unsigned long,
    unsigned long, unsigned long, unsigned long,
    bool, unsigned long, unsigned int, bool) ()
#7 0x0814158a in __asan_report_load1 ()
#8 0xf7e8bfbf in tt_cmap10_char_index (cmap=0xf4c00940,
    char_code=64)
    at /freetype-2.5.3/src/sfnt/ttmap.c:1931
#9 0xf7cdc271 in FT_Get_Char_Index (face=0xf4203c80,
    charcode=64)
    at /freetype-2.5.3/src/base/ftobjs.c:3347
#10 0x0817a5f3 in OutlinePrinter::LoadGlyph (this=
    <optimized out>, symbol=<optimized out>)
    at char2svg.cpp:246
#11 OutlinePrinter::Run (this=<optimized out>, symbol=
    <optimized out>) at char2svg.cpp:217
#12 0x0817d6f0 in main (argc=<optimized out>, argv=
    <optimized out>) at char2svg.cpp:486
```

(a) Full stack trace. The parts that are removed to obtain the coarse stack trace in Figure 2b are colored in green.

```
#0 0xf7fc4579 in __kernel_vsyscall
#1 0xf7799eb7 in ?? from /lib32/libc.so.6
#2 0xf77494c5 in raise from /lib32/libc.so.6
#3 0xf77323ac in abort from /lib32/libc.so.6
#4 0x0815f276 in __sanitizer::Abort
#5 0x0815d377 in __sanitizer::Die
#6 0x08138f8f in __asan::ReportGenericError
#7 0x0814158a in __asan_report_load1
#8 0xf7e8bfbf in tt_cmap10_char_index
    at /freetype-2.5.3/src/sfnt/ttmap.c:1931
#9 0xf7cdc271 in FT_Get_Char_Index
    at /freetype-2.5.3/src/base/ftobjs.c:3347
#10 0x0817a5f3 in OutlinePrinter::LoadGlyph
    at char2svg.cpp:246
#11 OutlinePrinter::Run at char2svg.cpp:217
#12 0x0817d6f0 in main at char2svg.cpp:486
```

(b) Coarse stack trace with all function arguments removed.

```
ERROR: AddressSanitizer: heap-buffer-overflow
on address 0xf4e0382a
at pc 0xf7e8bfbf bp 0xffffd8f8 sp 0xffffd8ec
READ of size 1 at 0xf4e0382a thread T0
Address 0xf4e0382a is a wild pointer.
SUMMARY: AddressSanitizer: heap-buffer-overflow
/freetype-2.5.3/src/sfnt/ttmap.c:1931:16
in tt_cmap10_char_index
```

(c) ASan report with removed stack trace, shadow map and legend.

Figure 2: Examples of data sources used by GPTrace. These were produced by the target char2svg.

distance is commonly used for LLM embedding vectors, it does not obey the triangle inequality. Several computations can be accelerated by using a distance function that does obey the triangle inequality, such as the Euclidean metric. When restricting to vectors that have a Euclidean norm of 1, the orderings of comparisons for the cosine distance and the Euclidean distance are the same. Thus, we normalize the final vectors with respect to the Euclidean metric and then use the Euclidean distance as our distance function in the subsequent steps. These combined, normalized vectors are now passed on to the clustering stage.

## 2.3 Clustering

Clustering algorithms generally provide parameters that control how coarse or fine-grained the resulting clusters are, requiring us to search for values that yield satisfactory results. This makes clustering algorithms that require the number of resulting clusters as a parameter, like  $k$ -means [20], unsuitable for our use case, since this value can range from 1 to the number of SCIs supplied to GPTrace, rendering a search impractical when analyzing a large number of crashing inputs. Moreover, we will see in Section 4.4 that  $k$ -means does not produce optimal results for our use case.

We found density-based clustering algorithms to provide good results for our application and since the arrangement and density of the embedding vectors is unknown and may vary both within a target as well as across different targets, we found a variable density clustering using HDBSCAN [3, 23, 24] to be more suitable than fixed density algorithms like DBSCAN [7]. HDBSCAN creates a cluster hierarchy and evaluates cluster stability over varying distance thresholds. It takes the parameters  $m_{clSize}$ , which determines the minimum number of points a cluster can have, and  $m_{pts}$ , which

influences how conservative the clustering will be. Large values of  $m_{pts}$  will result in many points declared as noise and only produce clusters in very dense areas. As there might well be only a single SCI for some bugs, we set these parameters as low as possible ( $m_{clSize} = 2$  and  $m_{pts} = 1$ ). Since this configuration is prone to creating a lot of micro-clusters, even in regions of high density, we use the hybrid approach by Malzer and Baum [22], which combines DBSCAN and HDBSCAN by using fixed density DBSCAN clusters below a distance threshold  $\epsilon$ , which is provided as a parameter.

In this setup,  $\epsilon$  is the main parameter that greatly influences the clustering result. GPTrace tries several values for  $\epsilon$  and chooses the one that produces the best clustering based on a strategy that we describe below. To achieve a time-efficient search for  $\epsilon$ , we devise Algorithm 1. Here, we limit the search interval to the range of distance values that actually occur in the dataset, skipping values that do not produce additional clusterings. Furthermore, we employ a divide-and-conquer approach to skip over  $\epsilon$ -ranges that leave the clustering unchanged. Since  $\epsilon$  only influences the final selection of the clustering from the cluster hierarchy, the computation of the minimum spanning tree of the mutual reachability graph can be done once, independently of  $\epsilon$ . This is the most time-consuming part of HDBSCAN and caching its result greatly improves the run time of the individual HDBSCAN runs and thereby of Algorithm 1.

The function *choose\_best\_clustering* used in Algorithm 1 quantifies the quality of each clustering produced by HDBSCAN and chooses the best one based on the following three metrics:

**Density Based Cluster Validity (DBCV):** DBCV [26] is a relative metric that uses values between  $-1$  and  $1$  to measure the quality of a clustering based on computing minimal density scores within clusters and maximal density scores between

---

**Algorithm 1:** GPTrace search algorithm for a good clustering. Here,  $min\_dist$  and  $max\_dist$  are the minimum and maximum distances between data points respectively.  $num\_steps$  specifies an upper limit on the number of iterations.

---

```

procedure cluster_search( $min\_dist, max\_dist, num\_steps$ )
  queue  $\leftarrow [(min\_dist, max\_dist)]$ 
  clusterings  $\leftarrow []$ 
  steps  $\leftarrow 0$ 
  while not_empty(queue) and steps < num_steps do
    ( $eps\_start, eps\_end$ )  $\leftarrow$  dequeue(queue)
    clustering_start  $\leftarrow$  hdbscan( $eps\_start$ )
    clustering_end  $\leftarrow$  hdbscan( $eps\_end$ )
    append(clusterings, clustering_start)
    append(clusterings, clustering_end)
    if clustering_start  $\neq$  clustering_end then
       $eps\_mid \leftarrow \frac{eps\_start + eps\_end}{2}$ 
      step  $\leftarrow \frac{eps\_mid - eps\_start}{num\_steps}$ 
      enqueue(queue, ( $eps\_start + step, eps\_mid$ ))
      enqueue(queue, ( $eps\_mid + step, eps\_end - step$ ))
    end
    steps  $\leftarrow$  steps + 1
  end
  return choose_best_clustering(clusterings)

```

---

pairs of clusters. DBCV is particularly suitable for quantifying the quality of density-based clusterings.

**Persistence:** The persistence of a clustering is a value between 0 and 1 that measures the distance range through which the clustering persists in the cluster hierarchy computed by HDBSCAN. We have found that clusterings with larger persistence values more closely resemble the ground truth.

**Number of clusters:** We count each point that HDBSCAN classifies as noise as a separate cluster. Although the number of clusters does not allow conclusions about the quality of the clustering itself, we prioritize clusterings with a lower number of clusters, as additional clusters result in potential manual work for humans. As fuzzing and bug fixing are iterative processes, a bug overlooked due to coarser clustering is likely to resurface in subsequent bug fixing rounds.

Based on these metrics, *choose\_best\_clustering* selects the best clustering from all candidates using the following strategy:

- (1) Record the largest DBCV score that occurs among all clusterings and then choose at most ten clusterings with the largest DBCV scores that deviate from the maximum recorded score by at most 20 %.
- (2) Among the resulting clusterings, record the largest persistence value and then choose all clusterings with persistence values that deviate from the maximum by at most 20 %.
- (3) Among the resulting clusterings, choose the one with the lowest number of clusters. Since the first two steps limit the deviation from the maximum DBCV score and persistence, only clusterings with acceptable accuracy will reach this step.

Thus, we select the clustering that minimizes the subsequent human analysis effort, as explained above.

The final result of GPTrace is a clustering of the supplied SCIs where each cluster is a group of SCIs that GPTrace suspects to have the same underlying bug.

### 3 Implementation

We implemented a prototype of GPTrace in Python 3.11. Although the general idea of GPTrace can be applied to deduplication of SCIs for programs written in any language, our prototype implementation targets C/C++ programs.

During development, we used OpenAI’s text-embedding-3-large model [30] for computing embeddings and we will discuss some specific adjustments we made in our implementation using the OpenAI Python library [29]. However, our prototype also supports SentenceTransformer [33] models, e.g., from Hugging Face [13].

The embedding vectors that text-embedding-3-large returns have a length of 3072. However, many clustering algorithms, including HDBSCAN, struggle with very-high dimensional data. Many state-of-the-art LLMs, including text-embedding-3-large, are trained using Matryoshka Representation Learning [18], a technique that produces embeddings where the first components of the vectors contain the most crucial information while the later components become more fine-grained. This allows us to truncate our embedding vectors to 64 dimensions without incurring significant loss of information. As these lower-dimensional vectors can be more easily handled by our clustering algorithm, this results in an overall gain in deduplication quality with a positive side-effect on run times.

Deduplication tools need to deal with large numbers of SCIs and sending individual embedding requests for the data of individual SCIs to the OpenAI API results in slow run times and rate limiting. To remedy this, we make use of OpenAI batch processing, which allows creating asynchronous jobs that consist of a large number of requests. To avoid computing embeddings multiple times during consecutive runs of GPTrace, we store the embeddings obtained by the LLM and label them using the hash of the data they belong to.

To achieve a fast clustering phase, we use the Python hdbscan library [24], which implements the hybrid clustering approach as well as caching minimum spanning trees as explained in Section 2.3.

Since GPTrace expects stack traces and ASan reports as input, we also provide a supplemental script that runs the binary with a set of SCIs (in parallel) and records the required data using GDB. Together, our GPTrace prototype and the data collection script allow developers to use our deduplication approach directly on crashing inputs gathered from fuzzing runs without any additional work. Furthermore, thanks to GPTrace’s modular design, the prototype can be easily adapted to further improve integration into real developing pipelines. For instance, fuzzing tools might support the collection of the required crash information (stack traces and ASan reports) during the fuzzing phase without the need to reproduce the crash at a later time. Moreover, since all steps except the final clustering can be done independently for each crashing input, it might make sense to split the GPTrace workflow into two parts: The first performs the preprocessing, computes the LLM embeddings and the final vectors, and is hooked up directly to the fuzzer output so that each crashing input is prepared right away. The second

part waits until all crashing inputs have been processed and then computes the final clustering.

## 4 Evaluation

In this section, we aim to answer the following questions:

- How well does GPTrace perform at crash deduplication?
- How does the choice of data sources impact the quality of deduplication results?
- Which clustering algorithms are suitable for our approach?
- How does the choice of LLM affect deduplication quality?
- How does GPTrace compare to existing state-of-the-art deduplication approaches?
- Do the underlying bug types influence the quality of deduplication results of GPTrace and other approaches?

We evaluated our prototype implementation on the ground truth SCI benchmark<sup>2</sup> created by the Igor [15] authors. It is based on the Magma [11] and MoonLight [12] benchmarks and contains 344 502 SCIs for 14 targets written in C/C++ with overall 61 ground truth labels grouping SCIs that are caused by the same bug. However, during their work on Igor, Jiang et al. found that some labels share the same root cause. Moreover, we noticed that one label (tiffcp: CVE201610269) only contains duplicate inputs that are also present under other labels (tiffcp: AAH013 and tiffcp: AAH014, both caused by CVE-2016-10269). We removed this ambiguous label and merged the duplicates identified by the Igor authors, yielding 341 952 inputs for 14 targets associated with 54 distinct ground truth labels.

In the benchmark, SCIs are grouped in directories named according to the corresponding ground truth label. Since the filename of an SCI is sometimes contained in the resulting stack traces, we flattened the directory structure and renamed all SCI files using generic file names to prevent leakage of ground truth information to the LLM, potentially (positively) disturbing the results.

During execution, some SCIs failed to reproduce the claimed crash. Out of the 54 distinct ground truth labels, we were not able to reproduce crashes for four of them (tiff2pdf: D, tiffcp: AAH015, xmlint: C and x509: AAH055). In the end, we collected a total of 327 071 stack traces and 325 044 ASan reports for 14 targets associated with 50 ground truth labels.

The experiments were carried out on a machine running Debian 12 (Linux 6.9) with two Intel Xeon Silver 4510 @ 4.10 GHz each with 12 cores, 512 GB of memory and an NVIDIA H100 NVL. Unless explicitly stated otherwise, we used text-embedding-3-large as LLM.

### 4.1 Evaluation Metrics

To get a better understanding of deduplication results, we use the ground truth labeling for each target to compute *purity*, *inverse purity* and *F-measure* as defined in [1]. We briefly recall the definitions of these measures in the context of our evaluation. Consider a fixed target program containing  $n$  bugs with ground truth labels  $l_1, \dots, l_n$  and suppose that  $N$  SCIs were supplied to GPTrace. Let

$$L_i := \{\text{data points that belong to ground truth label } l_i\}$$

for  $i = 1, \dots, n$ . Suppose further that  $c_1, \dots, c_m$  are the generated cluster labels and let

$$C_j := \{\text{data points that belong to cluster } c_j\},$$

for  $j = 1, \dots, m$ . We define the precision

$$\text{Precision}(L_i, C_j) := \frac{|L_i \cap C_j|}{|C_j|}$$

and recall

$$\text{Recall}(L_i, C_j) := \text{Precision}(C_j, L_i) = \frac{|L_i \cap C_j|}{|L_i|}$$

for the clustering  $C_1, \dots, C_m$ . The purity

$$\text{Purity} := \sum_{j=1}^m \frac{|C_j|}{N} \max_{i=1, \dots, n} \text{Precision}(L_i, C_j)$$

indicates whether data points in a cluster can be trusted to have the same underlying bug or whether data points with different underlying bugs are mixed into common clusters. The inverse purity

$$\text{InversePurity} := \sum_{i=1}^n \frac{|L_i|}{N} \max_{j=1, \dots, m} \text{Recall}(L_i, C_j)$$

on the other hand is a measure of how much data points with the same label are spread out across multiple clusters.

A method that always creates a new cluster for each SCI will achieve perfect purity scores of 100 %, whereas a method that consistently groups all SCIs into a single cluster will have perfect inverse purity scores of 100 %. Therefore, one always needs to consider both purity and inverse purity. The F-measure

$$\text{F-Measure} := \sum_{i=1}^n \frac{|L_i|}{N} \max_{j=1, \dots, m} \text{F}(L_i, C_j)$$

combines purity and inverse purity into a single metric for quantifying the quality of a deduplication method. Here,

$$\text{F}(L_i, C_j) := \frac{2 \text{Precision}(L_i, C_j) \text{Recall}(L_i, C_j)}{\text{Precision}(L_i, C_j) + \text{Recall}(L_i, C_j)},$$

for  $i = 1, \dots, n$ ,  $j = 1, \dots, m$ , where we set  $\text{F}(L_i, C_j) := 0$  in case both  $\text{Precision}(L_i, C_j)$  and  $\text{Recall}(L_i, C_j)$  vanish.

### 4.2 Results of GPTrace

We present the results of GPTrace per target in the evaluation dataset in the *All Data Sources* column of Table 1. They show that GPTrace predicts cluster counts close to the actual ground truth. We observe high and often perfect purity values, indicating that GPTrace rarely groups together SCIs with different underlying bugs. In practice, this allows developers to pick just one SCI from each cluster for further analysis without missing any of the bugs. High inverse purity scores suggest that in those cases where GPTrace produces too many clusters, those additional clusters mainly consist of a relatively small number of noisy SCIs while the vast majority of SCIs for each label is still concentrated in one main cluster. Thus, by analyzing single SCIs from the larger clusters, a developer is likely to cover all underlying bugs before reaching the smaller clusters that contain duplicate SCIs. Overall, GPTrace produces clusterings that very accurately resemble the ground truth labeling.

<sup>2</sup><https://github.com/HexHive/Igor?tab=readme-ov-file#ground-truth-benchmark>

**Table 1: GPTrace evaluation results for different choices of data sources using OpenAI’s text-embedding-3-large. Configurations: *All Data Sources* is our proposed approach for GPTrace combining full and coarse stack traces as well as ASan reports (see Section 2). *No Full Traces* uses coarse traces and ASan reports but no full traces. *No Coarse Traces* uses full traces and ASan reports but no coarse traces. *No ASan Reports* uses just the full and coarse traces but no ASan reports. *Only ASan Reports* uses just the ASan reports where the contained stack traces were not removed. *Bugs* gives the number of ground truth bugs. The *C* columns contain the number of clusters produced by the respective configurations. *P*, *IP*, and *F* denote purity, inverse purity, and F-measure, given in percentages rounded to the nearest integer. Best entries per target and metric are highlighted in green.**

Target	Bugs	All Data Sources				No Full Traces				No Coarse Traces				No ASan Reports				Only ASan Reports			
		C	P	IP	F	C	P	IP	F	C	P	IP	F	C	P	IP	F	C	P	IP	F
char2svg	6	8	100	98	99	12	100	86	92	9	100	98	99	7	93	98	91	9	100	98	99
client	1	1	100	100	100	1	100	100	100	1	100	100	100	1	100	100	100	5	100	95	98
exif	1	1	100	100	100	1	100	100	100	2	100	99	99	1	100	100	100	1	100	100	100
libxml2_xml_read_memory_fuzzer	1	1	100	100	100	1	100	100	100	1	100	100	100	1	100	100	100	1	100	100	100
pdf_fuzzer	2	2	100	100	100	2	100	100	100	2	100	100	100	2	100	100	100	2	100	100	100
pdfimages	4	5	100	96	98	5	100	96	98	4	100	100	100	4	100	100	100	5	100	96	98
pdftoppm	3	4	100	100	100	1	81	100	76	4	100	100	100	4	100	100	100	4	100	100	100
pdftotext	2	2	100	100	100	2	100	100	100	2	100	100	100	4	100	91	95	2	100	100	100
sox (mp3)	7	9	100	96	98	9	100	97	98	9	100	96	98	10	100	96	98	9	100	100	100
sox (wav)	5	8	100	56	71	8	100	56	71	8	100	56	72	9	100	56	71	9	100	56	71
tiff2pdf	3	5	100	97	98	3	99	100	99	36	100	91	94	5	100	97	98	4	100	100	100
tiffcp	6	6	85	99	89	6	85	99	89	6	85	99	88	7	85	97	88	6	85	99	89
x509	1	1	100	100	100	1	100	100	100	2	100	100	100	1	100	100	100	1	100	100	100
xmllint	8	22	83	74	68	29	83	72	67	1	78	100	74	1	79	100	74	1	79	100	74
Average			98	94	94		96	93	92		97	96	95		97	95	94		97	96	95

### 4.3 Effect of Choice of Data Sources

To assess how the selection of data sources affects deduplication quality, we used our proposed approach of combining *All Data Sources* as a baseline and then removed one of the data sources. The results are shown in the center three columns of Table 1. We also evaluated configurations that only use a single data source and found that out of those, the best deduplication quality is achieved when using *Only ASan Reports* (without removing the contained stack traces). The good results of this latter configuration indicate that relying solely on one data source can be sufficient for achieving accurate deduplication for many targets. Based on these results, there is only limited room for improvement when evaluating other GPTrace configurations and we see, in fact, that all assessed configurations can be used to deduplicate SCIs reliably. This indicates that the general approach of GPTrace is very flexible. We still propose combining *All Data Sources* for the following reasons: This configuration produces the highest purity values, indicating that clusters rarely include SCIs with different underlying bugs, thus proving the reliability of the bucketing for developers. In contrast, leaving out full stack traces decreases all three metrics for several targets. This suggests that the information contained in the full stack traces is valuable for deduplication and excludes the *No Full Traces* configuration as a viable alternative. Although removing coarse stack traces achieves good average metrics, it produces significantly worse results than our baseline for *tiff2pdf*, inaccurately producing the largest number of clusters in our comparison, and *xmllint*. For the latter target, while not optimal, our baseline pro-

duces a grouping that is acceptable for further analysis. Meanwhile, the *No Coarse Traces* configuration generates a single cluster that provides no information about the actual ground truth. The same incorrect single-cluster results for *xmllint* are also observed for the *No ASan Reports* and *Only ASan Reports* configurations and they artificially increase the average inverse purity of these configurations. In fact, *xmllint* is the sole reason why these achieve slightly better average inverse purity than our baseline configuration and excluding this target from the average rectifies this statistical effect. Overall, we see that, while the GPTrace method is able to produce very accurate bucketings using different selections of data sources, combining *All Data Sources* is the only configuration that achieves robust and usable results for all targets in our evaluation dataset.

### 4.4 Effect of Clustering Algorithm

We evaluated the performance of GPTrace when using different clustering algorithms and present the results in the three leftmost result columns of Table 2. We compared the *Hybrid HDBSCAN* [22] approach described in Section 2.3 with *DBSCAN* [7] and *k-means* [20]. As the DBCV [26] score is designed specifically for density-based clustering algorithms, we did not use it for *k-means* and instead relied on silhouette scores [34] in this case. Moreover, as mentioned earlier, *k-means* requires the number of clusters to be specified in advance and the correct value can reach from 1 to the number of SCIs. As the latter is very large for most of the targets in our dataset, we restrict the parameter search to a maximum of 100 clusters.



**Table 2: GPTrace evaluation results for different clustering algorithms and embedding models. Clustering algorithms: *Hybrid HDBSCAN* [22] as explained in Section 2.3, *DBSCAN* [7] and *k-means* [20]. Embedding models: *text-embedding-3-large* from OpenAI [30], *NV-Embed-v2* from NVIDIA [19] and *stella\_en\_1.5B\_v5* [41]. *Bugs* gives the number of ground truth bugs. The *C* columns contain the number of clusters produced by the respective configurations. *P*, *IP*, and *F* denote purity, inverse purity, and F-measure, given in percentages rounded to the nearest integer. Best entries per target and metric are highlighted in green. In the overlapping middle column, an entry is highlighted in lighter green with a mark in the bottom right corner if the configuration is the best among the embedding models but not among the clustering algorithms.**

Target	Bugs	DBSCAN				<i>k</i> -means				Hybrid HDBSCAN				text-emb.-3-large				NV-Embed-v2				stella_en_1.5B_v5			
		C	P	IP	F	C	P	IP	F	C	P	IP	F	C	P	IP	F	C	P	IP	F				
char2svg	6	8	100	98	99	2	72	100	73	8	100	98	99	8	100	98	99	7	93	98	91				
client	1	1	100	100	100	1	100	100	100	1	100	100	100	1	100	100	100	1	100	100	100				
exif	1	1	100	100	100	20	100	34	51	1	100	100	100	1	100	100	100	1	100	100	100				
libxml2_xml_read_memory_fuzzer	1	1	100	100	100	1	100	100	100	1	100	100	100	1	100	100	100	1	100	100	100				
pdf_fuzzer	2	2	100	100	100	2	100	100	100	2	100	100	100	2	100	100	100	2	100	100	100				
pdfimages	4	5	100	96	98	3	81	100	87	5	100	96	98	4	96	96	96	4	96	96	96				
pdftoppm	3	4	100	100	100	3	100	100	100	4	100	100	100	4	100	100	100	4	100	100	100				
pdftotext	2	5	100	87	92	2	100	100	100	2	100	100	100	4	100	91	95	1	85	100	82				
sox (mp3)	7	10	100	96	98	9	100	96	98	9	100	96	98	10	100	96	98	10	100	96	98				
sox (wav)	5	10	100	56	71	6	100	99	100	8	100	56	71	8	100	56	71	8	100	56	71				
tiff2pdf	3	6	100	97	98	3	99	100	99	5	100	97	98	5	100	100	100	1	93	100	90				
tiffcp	6	6	85	99	89	4	67	100	70	6	85	99	89	7	85	97	88	9	85	87	85				
x509	1	1	100	100	100	1	100	100	100	1	100	100	100	1	100	100	100	1	100	100	100				
xmllint	8	1	79	100	74	6	83	77	69	22	83	74	68	1	79	100	74	1	79	100	74				
Average			97	95	94		93	93	89		98	94	94		97	95	94		95	95	92				

Both DBSCAN and HDBSCAN produce good results for most targets, but overall the results favor HDBSCAN, which is more accurate for several targets (e.g., *pdftotext* and *tiff2pdf*). While *k*-means also yields acceptable deduplication quality, the average metrics indicate a noticeably worse performance than the density-based clustering approaches. Depending on the target, we observe problems regarding both purity (e.g., *char2svg* and *tiffcp*) and inverse purity (e.g., *exif*) of the produced bucketings. Combined with the practical difficulty of searching for the best number of clusters, this suggests that, as suspected, *k*-means is not suitable for our use case.

#### 4.5 Effect of Choice of Embedding Model

In addition to using OpenAI’s *text-embedding-3-large* model, we also evaluated LLMs that can be run locally. We chose NVIDIA’s *NV-Embed-v2* [19] because it is among the highest-ranking models on the Massive Text Embedding Benchmark (MTEB) leaderboard [27] (as of January 13, 2025), which ranks the performance of embedding models across different tasks. We also tried *stella\_en\_1.5B\_v5* [41] because it ranks high on the MTEB leaderboard as well while being substantially smaller (~1.5 B parameters) than NVIDIA’s *NV-Embed-v2* (~8 B parameters) and thus suitable for less powerful hardware.

The three rightmost columns of Table 2 show that for most targets all three models produce good estimates of the ground truth, indicating that GPTrace can be used with different LLMs. However, we see some decline in deduplication quality when using the smaller

*stella\_en\_1.5B\_v5* model suggesting that GPTrace can profit from larger models like *text-embedding-3-large* or *NV-Embed-v2*.

The target where the difference between the evaluated models is most noticeable is *xmllint*. While the results generated using *text-embedding-3-large* remain reasonably accurate, both *NV-Embed-v2* and *stella\_en\_1.5B\_v5* produce poor results. The SCIs for *xmllint* generate long execution paths, many of which differ only marginally even across ground truth labels. The results in Section 4.6 suggest

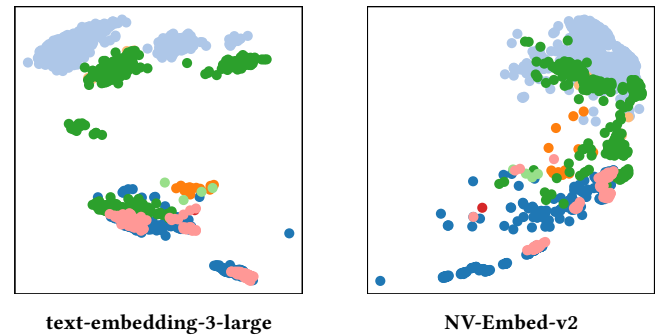


**Figure 3: Two-dimensional projections of the combined vectors for *xmllint*, obtained using scikit-learn’s [2, 31] truncated singular value decomposition. The colors indicate the eight different ground truth labels.**

**Table 3: Deduplication results of GPTrace in comparison to Crashwalk [28], our implementation of DeFault [42], and Igor [15]. Bugs gives the number of ground truth bugs. The C columns contain the number of clusters produced by the respective configurations. P, IP, and F denote purity, inverse purity, and F-measure, given in percentages rounded to the nearest integer. Best entries per target and metric are highlighted in green.**

Target	Bugs	GPTrace				Crashwalk				DeFault				Igor			
		C	P	IP	F	C	P	IP	F	C	P	IP	F	C	P	IP	F
char2svg	6	8	100	98	99	67	100	61	73	2	37	99	46	3	33	91	34
client	1	1	100	100	100	1	100	100	100	1	100	100	100	1	100	100	100
exif	1	1	100	100	100	121	100	32	49	2	100	100	100	2	100	61	76
libxml2_xml_read_memory_fuzzer	1	1	100	100	100	99	100	11	20	1	100	100	100	3	100	38	55
pdf_fuzzer	2	2	100	100	100	10	100	54	68	1	72	100	73	2	100	100	100
pdfimages	4	5	100	96	98	21	100	86	90	5	46	87	45	6	87	72	78
pdftoppm	3	4	100	100	100	6	100	100	100	4	82	83	78	3	65	81	67
pdftotext	2	2	100	100	100	10	100	88	91	2	93	97	91	3	90	56	62
sox (mp3)	7	9	100	96	98	18	100	96	98	2	92	97	87	2	42	99	51
sox (wav)	5	8	100	56	71	15	100	55	71	1	95	100	93	2	60	100	68
tiff2pdf	3	5	100	97	98	7	100	89	94	1	93	100	91	2	49	72	56
tiffcp	6	6	85	99	89	12	85	74	76	4	59	91	63	6	89	90	89
x509	1	1	100	100	100	1	100	100	100	1	100	100	100	1	100	100	100
xmllint	8	22	83	74	68	825	84	18	28	1	79	100	75	4	70	98	76
Average			98	94	94		98	69	76		82	97	82		78	83	72

that this also poses a problem for other deduplication approaches. While text-embedding-3-large still extracts distinguishing information from the coarse stack traces, this information does not seem pronounced enough in the embeddings from NV-Embed-v2 and stella\_en\_1.5B\_v5. This limitation persists in the combined embeddings, as can be seen in the two-dimensional projections in Figure 3. Consequently, GPTrace produces useful clusters with text-embedding-3-large but fails to do so with the other models.

The choice of LLM also impacts the run time of GPTrace. Using OpenAI’s batch API, results of embedding requests are claimed to be returned within 24 hours. In practice, we have experienced significantly shorter turnaround times, ranging from under a minute to a few hours, depending on the number of embeddings requested. Still, gathering embeddings constitutes the majority of GPTrace’s run time. This is evidently influenced by OpenAI’s capacity at the time of the request and while we did not perform a systematic evaluation, we observed that deduplicating the entire dataset corresponding to 327 071 SCIs using text-embedding-3-large is possible in less than ten hours. In contrast, utilizing a local LLM on suitable hardware significantly reduces run times. On our evaluation machine, deduplication with stella\_en\_1.5B\_v5 takes only 41 minutes, while using NV-Embed-v2 reduces the run time to 39 minutes.

#### 4.6 Comparison to Existing Deduplication Methods

Having determined the best-performing configuration for GPTrace, we now compare its performance to that of Crashwalk [28], which serves as a representative of stack hashing approaches, DeFault [42], which groups crashes based on mutual information scores of the basic blocks present in their execution traces, and Igor [15], which

compares minimized control flow graphs of crashes. We do this by, again, collecting the number of clusters as well as purity, inverse purity and F-measure. The results are presented in Table 3.

Crashwalk records stack traces of SCIs and groups together those inputs whose stack traces have the same hash value. We see from the results in Table 3 that, compared to Crashwalk, GPTrace provides more accurate deduplication results across almost all targets. Since crashes that result from different bugs are unlikely to produce identical stack traces, Crashwalk is able to distinguish between different bugs very well, as is expressed by its high purity scores. However, even small differences in the stack traces lead to different hash values and Crashwalk has no way of capturing such nuances. This results in a lot of duplicate buckets for the same bug and hence lower inverse purity scores. GPTrace, on the other hand, can take account of the similarity of both stack traces as well as further information from the supplied ASan reports. This leads to considerably higher inverse purity scores by virtue of lower numbers of clusters that are much closer to the ground truth.

DeFault requires as input the basic block-level execution traces of the crashing SCIs and of non-crashing inputs. It then identifies basic blocks that have high mutual information scores related to crashing behavior and groups the SCIs based on which basic blocks their traces contain. As the source code for DeFault is not publicly available, we implemented a prototype ourselves based on the paper’s description, focusing solely on the deduplication mechanism while excluding unrelated components, such as fault localization.<sup>3</sup> We then generated non-crashing inputs using AFL/AFL++ [8, 40] and collected basic block traces using Intel Pin [21]. The results

<sup>3</sup>Our prototype implementation of DeFault is contained in our artifact repository at <https://github.com/Fraunhofer-AISEC/gptrace-artifacts>.



**Table 4: Results of GPTrace, Crashwalk [28], our implementation of DeFault [42], and Igor [15] for different bug types classified by their CWE Type [37]. The Total column contains the number of bugs of each type. Over columns contain the mean ( $\mu$ ) and standard deviation ( $\sigma$ ) of the overcounting scores for the respective bug types while Under columns contain the mean and standard deviation of the undercounting scores, all rounded to one decimal place. Apparent outliers are highlighted in red.**

CWE Type	Total	GPTrace				Crashwalk				DeFault				Igor			
		Over		Under		Over		Under		Over		Under		Over		Under	
		$\mu$	$\sigma$	$\mu$	$\sigma$	$\mu$	$\sigma$	$\mu$	$\sigma$	$\mu$	$\sigma$	$\mu$	$\sigma$	$\mu$	$\sigma$	$\mu$	$\sigma$
Improper Restriction of Operations within the Bounds of a Memory Buffer	28	1.1	2.7	0.6	1.0	46.3	89.1	0.5	0.7	0.5	0.8	4.4	2.2	0.8	0.9	2.8	1.7
Out-of-bounds Read	11	0.3	0.7	0.2	0.4	15.2	35.7	0.2	0.4	1.1	0.9	3.3	1.7	1.2	1.0	2.5	1.6
Out-of-bounds Write	6	0.3	0.5	0.8	1.0	1.7	0.8	0.8	1.0	0.3	0.8	4.8	1.0	0.2	0.4	3.3	1.4
Other	11	2.3	4.0	1	1.3	101.6	120.5	0.6	0.7	0	0.0	5.3	2.7	0.6	0.8	2.8	2.0
Incorrect Calculation	11	0.6	0.9	0.6	0.8	14.7	35.2	0.6	0.8	0.5	0.9	3.4	2.2	0.5	0.7	2	1.7
Integer Overflow or Wraparound	10	0.6	1.0	0.7	0.8	16.1	36.8	0.6	0.8	0.5	1.0	3.3	2.3	0.5	0.7	2.1	1.8
Divide By Zero	1	1	0	0	0	1	0	0	0	0	0	4	0	0	0	1	0
NULL Pointer Dereference	6	1	1.6	0.7	0.8	2.7	2.3	0.5	0.8	0.3	0.5	4.3	2.1	0.2	0.4	2.7	2.1
Other	15	0.5	1.1	0.7	1.4	1.5	1.5	0.5	0.7	0.8	1.2	3.8	2.1	0.6	0.7	2.3	1.6
Total	60	0.8	2.0	0.7	1.0	24.9	65.3	0.5	0.7	0.6	0.9	4.1	2.2	0.6	0.8	2.5	1.7

show that DeFault is not able to provide deduplication results that are as accurate as those of GPTrace. While inverse purity scores are high, this is, again, often due to the small number of clusters produced by DeFault, typically less than the number of ground truth labels. This also leads to groups of SCIs with different underlying bugs, resulting in low purity scores.

Igor is a deduplication method that collects minimized control flow graphs of SCIs and clusters them based on graph similarity metrics. We evaluated Igor using the available prototype implementation and used a running time of 15 minutes per SCI for the minimum-coverage fuzzing phase as recommended by the authors. As Igor’s clustering algorithm is only capable of producing results with at least two clusters, the authors suggest comparing their results to those of a stack trace hashing approach, and choosing the result that produces the smaller number of clusters. We followed this recommendation leading to improved results for *client* and *x509*. For the other two single-bug targets, however, stack trace hashing generates far too many clusters, making this strategy ineffective. Even though Igor’s results in these cases are still acceptable, they do not recover the ground truth as reliably as GPTrace. Igor’s deduplication also falls short for many of the other targets, suffering from both low purity and inverse purity scores. In general, Igor’s results are not as accurate as those of GPTrace.

Apart from improved deduplication quality, GPTrace also has the advantage of requiring less data that is easier to obtain, compared to Igor and DeFault. While GPTrace only needs stack traces and ASan reports, both of which can easily be collected during the fuzzing process, the other approaches both require the collection of full execution traces. These cannot be generated as part of the fuzzing process, as this would add considerable overhead. Furthermore, these full execution traces are oftentimes very large (the Igor authors report sizes of up to 10 GiB for a single trace), potentially leading to difficulties in storing them and causing long run times of the deduplication tools. The problem of long run times is espe-

cially relevant for Igor, whose aforementioned minimum-coverage fuzzing phase is recommended by the authors to run for 15 minutes per SCI. On our dataset, this phase alone would require close to 4000 CPU hours and thus multiple days on our evaluation machine.

#### 4.7 Influence of Bug Type

In order to determine if the types of the underlying bugs influence the deduplication quality of GPTrace and the other approaches, we gathered the CWE [37] classifications of the bugs in our evaluation dataset, according to their CVE entries [36], and collected how the SCIs corresponding to each of the bugs are bucketed by the various deduplication methods. We present the results in Table 4 where we measure the deduplication quality for individual bugs by over- and undercounting scores. Given a ground truth label  $l$ , the overcounting score

$$\text{Overcounting}(l) := |\{\text{clusters containing an SCI from } l\}| - 1$$

measures how many superfluous clusters are created for the label  $l$ , while the undercounting score

$$\text{Undercounting}(l) := \left| \left\{ \begin{array}{l} \text{labels } l' \neq l \text{ for which some SCI} \\ \text{shares a cluster with an SCI from } l \end{array} \right\} \right|$$

counts how many other labels are grouped together into clusters with  $l$ . Scores close to zero indicate accurate deduplication.

The results show, again, that Crashwalk tends to produce a large number of clusters for each ground truth label, leading to very pronounced overcounting, while DeFault and Igor generate too few clusters, leading to undercounting. Meanwhile, GPTrace achieves balanced groupings with low over- and undercounting.

Looking at the results of GPTrace for specific bug types, we see that over- and undercounting scores are similar between bug types with the exception of *Other* bugs of the Type *Improper Restriction of Operations within the Bounds of a Memory Buffer* (highlighted in red in Table 4), where overcounting is significantly more prevalent than

for other bug types. The reason for this is that out of the 11 bugs of this category, 6 come from the xmlint target where GPTrace generates a fairly large number of clusters. If the bugs from xmlint are excluded, this outlier effect disappears (Over:  $\mu = 0$ ,  $\sigma = 0$ ; Under:  $\mu = 0.4$ ,  $\sigma = 0.89$ ), suggesting that there is no clear correlation between the underlying bug type and the quality of GPTrace’s deduplication results. Instead, the outlier is a consequence of the specific behavior of xmlint that we discussed in Section 4.5.

The mean over- and undercounting scores computed for Crashwalk vary significantly between bug types. However, the oftentimes very large standard deviations indicate that there is also significant variance within the bug types. In fact, among the three bug types that show the most overcounting (highlighted in red in Table 4), a small number of bugs (nine out of 32) is responsible for the majority of the overcounting while the remaining ones produce scores that are similar to those of other bug types. This suggests that the deduplication results of Crashwalk are also not immediately influenced by the underlying bug type. Rather, due to the rigid nature of stack trace hashing, Crashwalk’s results exhibit a lot of overcounting for bugs that produce even marginally different stack traces. This will be especially prominent in cases where the same bug triggers crashes through many different execution paths, as is the case for the aforementioned bugs that contribute most to the overcounting.

For DeFault and Igor, over- and undercounting is similar across different bug types, indicating that their deduplication results are not significantly influenced by the underlying bug type either.

#### 4.8 Threats to Validity

One main factor that could influence the general quality of our results is the choice of targets in our evaluation. Namely, all targets in our evaluation dataset are C/C++ programs. While the method of GPTrace is applicable to data sources from programs written in any language, we cannot ensure that the results in this case will have the same quality as in our evaluation of C/C++ targets. Moreover, even though we used the existing Igor dataset (which is itself based on the well-established Magma [11] and MoonLight [12] benchmarks) and did not specifically pick the targets for our evaluation, the quality of GPTrace’s results across a larger dataset might vary depending on the programs and contained bugs that are under test.

Related to this is the fact that the targets in the evaluation dataset are well-known software projects and information related to them has likely been contained in the training sets of the LLMs that we used in our evaluation. This could influence the quality of GPTrace’s deduplication results for new, unknown targets.

### 5 Related Work

This section gives an overview of existing deduplication approaches and we compare important aspects of these in Table 5. As GPTrace analyzes readily available crash information, such as stack traces and ASan reports, we divide the approaches based on whether they use similar information [6, 9, 17, 25, 28, 35, 39] or whether they require more detailed information about the full program execution [5, 15, 32, 42] or are based on other principles [16, 38]. There is also work on using LLMs to solve the related problem of triaging and deduplicating bug reports that are written and submitted by humans on bug tracking portals [4, 14]. Since this

**Table 5: Comparison of GPTrace and other deduplication approaches.**

Deduplication Method	Design			Implementation	
	Data Source	Grouping Method	Arbitrary Bug Types	Available Online	Target Language
GPTrace	Basic	Cluster	✓	✓	C/C++
DeFault [42]	ExInfo	Custom	✓	-	Binary
FuzzerAid [16]	ModBin	Repro	✓	-	C/C++
Igor [15]	ExInfo	Cluster	✓	✓	Binary
Modani et al. [25]	Basic	Custom	✓	-	C/C++
Pham et al. [32]	ExInfo	Custom	✓	-	LLVM
ReBucket [6]	Basic	Cluster	✓	*	C/C++
RETracer [5]	ExInfo	Custom	-	-	Binary
S3M [17]	Basic	-	✓	✓	Java
Trace Hashing [9, 28, 35]	Basic	Equal	✓	✓	C/C++
TraceSim [39]	Basic	-	✓	✓	Java
Van Tonder et al. [38]	ModBin	Repro	-	✓	C/C++
Basic	Ordinary crash information, e.g., stack traces or ASan reports				
ExInfo	Separate, detailed information gathered during execution, e.g., full execution traces or data gathered during symbolic execution				
ModBin	Modified binary for each SCI				
Cluster	Common clustering algorithm				
Custom	Custom grouping algorithm				
Equal	Check for strict equality				
Repro	Use (non-)reproduction of crash with modified binaries as oracle				
*	Only unofficial, incomplete implementations available				

problem is rather different from our fuzzing use case, we will not go into more detail here.

*Deduplication Using Basic Crash Information.* Stack trace-based deduplication approaches collect, for each SCI, the stack trace at the time the program crashes and use this information to group the SCIs. Since analysis of these stack traces can often be done very efficiently, these approaches tend to be quite fast.

One very simple, yet widely used way of stack trace-based deduplication is computing hash values of stack traces and grouping together all SCIs that produce the same hash value. As even small changes in the stack traces lead to different hash values, this approach often creates many groups for SCIs that have the same underlying bug. The results can be somewhat improved by ignoring function arguments in the stack traces, but the tendency to produce results with low inverse purity scores remains, as we have seen in Section 4.6. This causes additional manual work in real fuzzing workflows. Existing tools that employ this method differ in whether they include the entire stack trace in the computation of the hash value, like Crashwalk [28] and afl-collect [35], or only use some of the topmost stack frames, such as Honggfuzz [9].

To improve on these hash-based approaches, other deduplication methods develop more nuanced notions of similarity of stack traces. Modani et al. [25] use primitive string metrics, such as the Levenshtein distance or the Longest Common Subsequence algorithm, to compute similarity scores of stack traces. An incoming crash is

then assigned to the bucket that contains the trace with the highest similarity score unless a pre-defined lower limit is not surpassed, in which case a new bucket is created. TraceSim [39] also compares stack traces based on Levenshtein distances but tries to improve the results by using frame weights to focus on those frames that help the most in determining duplicate crashes. To find good weights, they employ a suitable metric, which they optimize using machine learning techniques. ReBucket [6] uses a simple algorithm that parses pairs of stack traces, compares which functions occur at what positions inside them and computes a score based on this data. The crash bucketing is then obtained by applying a hierarchical clustering algorithm. In comparison to GPTrace, these approaches extract only limited syntactic information from the stack traces that is often prone to being disturbed. For instance, methods that use primitive string metrics, such as the Levenshtein distance, can yield inaccurate results if multiple distinct functions have names that are syntactically similar, e.g., `beginPass` and `beginParse`.

The stack trace analysis approach that is most similar to ours is S3M [17]. The authors propose tokenizing stack traces using a dictionary of previously seen tokens and training a neural network that creates vector representations of these tokenized stack traces. Using these vectors, S3M computes for each pair of stack traces a three-dimensional feature vector, which is then fed into another neural network that computes a final similarity score. In contrast to GPTrace, S3M works with Java Virtual Machine (JVM) traces and does not leverage the large amount of information that state-of-the-art LLMs learn during their training. Moreover, their use of a second neural network for computing similarity scores from feature vectors makes S3M less transparent and they do not propose a method that groups the SCIs based on those similarity scores.

*Other Deduplication Approaches.* There are also deduplication methods that do not (solely) analyze stack traces or other basic crash data. Often, these approaches monitor or manipulate the execution of each SCI to gather additional information that is not captured by ordinary stack traces and use it to produce deduplication results.

RETracer [5] performs binary analysis based on memory dumps to find the root cause of crashes. However, it is limited in the types of crashes it can analyze and its target use case is crash triage based on limited information that is collected on end user machines rather than active software testing through fuzzing. Pham et al. [32] use symbolic execution to capture semantic information of different execution paths, which is then used to group SCIs. While GPTrace focuses on deduplicating crashes returned by a fuzzing campaign, Pham et al. aim to assist developers in debugging software by collecting information about the semantics of the program. Furthermore, being based on symbolic execution, their method is prone to long run times, especially for large real-world programs. The method developed by Van Tonder et al. [38] creates approximate bug fixes and groups SCIs together if they can be caught by the same approximate bug fix. This approach is very limited in the types of bugs it can handle since the required approximate bug fixes strongly depend on the bug type and need to be written manually. This is incompatible with the real-world deduplication use case that GPTrace targets. FuzzerAid [16] extracts for each SCI a fault signature, i.e., a small selection of statements from the original program that is necessary to reproduce the crash. If one input leads

to a crash of another input's fault signature, then these two inputs are grouped together. Unfortunately, we cannot compare GPTrace's deduplication capabilities to FuzzerAid's, as there is no source code of FuzzerAid publicly available and the evaluation in the paper is based on a different dataset than ours.

DeFault [42] quantifies the relevance of basic blocks of execution traces to crashing behavior by computing mutual information scores. These are a measure of how likely an execution trace is to correspond to a crash given that it contains a specific basic block. To do this, they also include non-crashing traces in their analysis. The authors then devise an algorithm that groups SCIs based on the mutual information scores of their associated stack traces. Since there is no source code available for DeFault, we implemented a prototype implementation based on the paper's description and the evaluation showed that it cannot produce results that are as accurate as those of GPTrace. Igor [15] clusters SCIs based on the similarity of control flow graphs. To improve the deduplication quality, Igor does not use the control flow graphs that are directly associated to the SCIs but instead introduces a minimum-coverage fuzzing phase that finds another SCI that still triggers the same bug but does so via an execution path that is as short as possible. As we have seen in Section 4.6, Igor produces deduplication results that are not as accurate as those of GPTrace and introduces complexity as well as long run times when integrated into real fuzzing workflows.

## 6 Conclusion and Future Work

The large amounts of data collected during fuzzing campaigns can quickly become overwhelming and waste valuable human resources. To remedy this, we presented and implemented GPTrace, an approach that uses LLM embeddings of crashing data to deduplicate SCIs. We evaluated GPTrace on a large dataset and have seen that it produces more accurate deduplication results than stack trace hashing approaches and even more complex state-of-the-art deduplication methods that require longer run times. To enable reproducibility of our results and facilitate future research, we make our GPTrace implementation and artifacts publicly available.

There are two directions of future work that might enable improvements of GPTrace. First, it would be interesting to investigate what further data sources beyond stack traces and ASan reports carry meaningful information about crashing behavior. Thanks to the flexible design of GPTrace, these could be integrated into GPTrace and enable better deduplication for targets that prove challenging when relying solely on stack traces and ASan reports. Secondly, while the general LLMs that we evaluated already produce embeddings that yield good deduplication results, it would be interesting to investigate whether specifically fine-tuning LLMs on the task of deduplication leads to even more accurate bucketings.

## Acknowledgments

We would like to thank the anonymous reviewers for their valuable suggestions for improving this paper. This research was supported by the Bavarian Ministry of Economic Affairs, Regional Development and Energy.

## References

- [1] Enrique Amigó, Julio Gonzalo, Javier Artiles, and Felisa Verdejo. 2009. A Comparison of Extrinsic Clustering Evaluation Metrics Based on Formal Constraints. *Information Retrieval* 12, 4 (Aug. 2009), 461–486. doi:10.1007/s10791-008-9066-8
- [2] Lars Buitinck, Gilles Louppe, Mathieu Blondel, Fabian Pedregosa, Andreas Mueller, Olivier Grisel, Vlad Niculae, Peter Prettenhofer, Alexandre Gramfort, Jaques Grobler, Robert Layton, Jake VanderPlas, Arnaud Joly, Brian Holt, and Gaël Varoquaux. 2013. API Design For Machine Learning Software: Experiences from the scikit-learn Project. In *2013 Languages for Data Mining and Machine Learning Workshop at European Conference on Machine Learning and Principles and Practice of Knowledge Discovery in Databases (LML '13)*. Workshop on Languages for Data Mining and Machine Learning, Prague, Czech Republic, 108–122.
- [3] Ricardo J. G. B. Campello, Davoud Moulavi, and Joerg Sander. 2013. Density-Based Clustering Based on Hierarchical Density Estimates. In *Advances in Knowledge Discovery and Data Mining (PAKDD '13, Vol. 7819)*. Springer Berlin Heidelberg, Berlin, Heidelberg, 160–172. doi:10.1007/978-3-642-37456-2\_14
- [4] Christopher A. Choquette-Choo, David Sheldon, Jonny Proppe, John Alphonso-Gibbs, and Harsha Gupta. 2019. A Multi-label, Dual-Output Deep Neural Network for Automated Bug Triaging. In *2019 18th IEEE International Conference On Machine Learning And Applications (ICMLA '19)*. IEEE, Boca Raton, USA, 937–944. doi:10.1109/ICMLA.2019.00161
- [5] Weidong Cui, Marcus Peinado, Sang Kil Cha, Yanick Fratantonio, and Vasileios P. Kemerlis. 2016. RETracer: Triaging Crashes by Reverse Execution From Partial Memory Dumps. In *Proceedings of the 2016 38th International Conference on Software Engineering (ICSE '16)*. ACM, Austin, USA, 820–831. doi:10.1145/2884781.2884844
- [6] Yingnong Dang, Rongxin Wu, Hongyu Zhang, Dongmei Zhang, and Peter Nobel. 2012. ReBucket: A Method for Clustering Duplicate Crash Reports Based on Call Stack Similarity. In *Proceedings of the 2012 34th International Conference on Software Engineering (ICSE '12)*. IEEE, Zurich, Switzerland, 1084–1093. doi:10.1109/ICSE.2012.6227111
- [7] Martin Ester, Hans-Peter Kriegel, Jörg Sander, and Xiaowei Xu. 1996. A Density-Based Algorithm for Discovering Clusters in Large Spatial Databases with Noise. In *Proceedings of the 1996 Second International Conference on Knowledge Discovery and Data Mining (KDD '96)*. AAAI Press, Portland, USA, 226–231.
- [8] Andrea Fioraldi, Dominik Maier, Heiko Eißfeldt, and Marc Heuse. 2020. AFL++: Combining Incremental Tests of Fuzzing Research. In *Proceedings of the 2020 14th USENIX Workshop on Offensive Technologies (WOOT '20)*. USENIX Association, Virtual, USA, 1–12. <https://www.usenix.org/conference/woot20/presentation/fioraldi>
- [9] Google. 2010. *Honggfuzz*. Retrieved Jan. 13, 2025 from <https://honggfuzz.dev>
- [10] Google. 2012. *AddressSanitizer*. Retrieved Jan. 13, 2025 from <https://github.com/google/sanitizers/wiki/AddressSanitizer>
- [11] Ahmad Hazimeh, Adrian Herrera, and Mathias Payer. 2020. Magma: A Ground-Truth Fuzzing Benchmark. *Proceedings of the ACM on Measurement and Analysis of Computing Systems* 4, 3 (Nov. 2020), 1–29. doi:10.1145/3428334
- [12] Adrian Herrera, Hendra Gunadi, Shane Magrath, Michael Norrish, Mathias Payer, and Antony L. Hosking. 2021. Seed Selection for Successful Fuzzing. In *Proceedings of the 2021 30th ACM SIGSOFT International Symposium on Software Testing and Analysis (ISSTA '21)*. ACM, Virtual, Denmark, 230–243. doi:10.1145/3460319.3464795
- [13] Hugging Face. 2016. *Hugging Face*. Retrieved Jan. 13, 2025 from <https://huggingface.co>
- [14] Yuan Jiang, Xiaohong Su, Christoph Treude, Chao Shang, and Tiantian Wang. 2023. Does Deep Learning Improve the Performance of Duplicate Bug Report Detection? An Empirical Study. *Journal of Systems and Software* 198 (April 2023), 111607. doi:10.1016/j.jss.2023.111607
- [15] Zhiyuan Jiang, Xiyue Jiang, Ahmad Hazimeh, Chaojing Tang, Chao Zhang, and Mathias Payer. 2021. Igor: Crash Deduplication Through Root-Cause Clustering. In *Proceedings of the 2021 ACM SIGSAC Conference on Computer and Communications Security (CCS '21)*. ACM, Virtual Event, Republic of Korea, 3318–3336. doi:10.1145/3460120.3485364
- [16] Ashwin Kallingal Joshy and Wei Le. 2022. FuzzerAid: Grouping Fuzzed Crashes Based On Fault Signatures. In *Proceedings of the 2022 37th IEEE/ACM International Conference on Automated Software Engineering (ASE '22)*. ACM, Rochester, USA, 1–12. doi:10.1145/3551349.3556959
- [17] Aleksandr Khvorov, Roman Vasiliev, George Chernishev, Irving Muller Rodrigues, Dmitriy Koznov, and Nikita Povarov. 2021. S3M: Siamese Stack (Trace) Similarity Measure. In *Proceedings of the 2021 IEEE/ACM 18th International Conference on Mining Software Repositories (MSR '21)*. IEEE, Madrid, Spain, 266–270. doi:10.1109/MSR52588.2021.00038
- [18] Aditya Kusupati, Gantavya Bhatt, Aniket Rege, Matthew Wallingford, Aditya Sinha, Vivek Ramanujan, William Howard-Snyder, Kaifeng Chen, Sham Kakade, Prateek Jain, and Ali Farhadi. 2022. Matryoshka Representation Learning. In *Proceedings of the 2022 36th International Conference on Neural Information Processing Systems (NeurIPS '22)*. Curran Associates Inc., Red Hook, NY, USA, Article 2192, 17 pages.
- [19] Chankyu Lee, Rajarshi Roy, Mengyao Xu, Jonathan Raiman, Mohammad Shoeybi, Bryan Catanzaro, and Wei Ping. 2025. NV-Embed: Improved Techniques for Training LLMs as Generalist Embedding Models. arXiv:2405.17428
- [20] Stuart Lloyd. 1982. Least Squares Quantization in PCM. *IEEE Transactions on Information Theory* 28, 2 (March 1982), 129–137. doi:10.1109/tit.1982.1056489
- [21] Chi-Keung Luk, Robert Cohn, Robert Muth, Harish Patil, Artur Klauser, Geoff Lowney, Steven Wallace, Vijay Janapa Reddi, and Kim Hazelwood. 2005. Pin: Building Customized Program Analysis Tools with Dynamic Instrumentation. In *Proceedings of the 2005 ACM SIGPLAN Conference on Programming Language Design and Implementation (PLDI '05)*. ACM, Chicago, USA, 190–200. doi:10.1145/1065010.1065034
- [22] Claudia Malzer and Marcus Baum. 2020. A Hybrid Approach To Hierarchical Density-based Cluster Selection. In *2020 IEEE International Conference on Multi-sensor Fusion and Integration for Intelligent Systems (MFI '20)*. IEEE, Karlsruhe, Germany, 223–228. doi:10.1109/MFI49285.2020.9235263
- [23] Leland McInnes and John Healy. 2017. Accelerated Hierarchical Density Based Clustering. In *2017 IEEE International Conference on Data Mining Workshops (ICDMW '17)*. IEEE, New Orleans, USA, 33–42. doi:10.1109/ICDMW.2017.12
- [24] Leland McInnes, John Healy, and Steve Astels. 2017. Hdbscan: Hierarchical Density Based Clustering. *The Journal of Open Source Software* 2, 11 (March 2017), 205. doi:10.21105/joss.00205
- [25] Natwar Modani, Rajeev Gupta, Guy Lohman, Tanveer Syeda-Mahmood, and Laurent Mignet. 2007. Automatically Identifying Known Software Problems. In *2007 IEEE 23rd International Conference on Data Engineering Workshop (ICDE '07)*. IEEE, Istanbul, Turkey, 433–441. doi:10.1109/ICDEW.2007.4401026
- [26] Davoud Moulavi, Pablo A. Jaskowiak, Ricardo J. G. B. Campello, Arthur Zimek, and Jörg Sander. 2014. Density-Based Clustering Validation. In *Proceedings of the 2014 SIAM International Conference on Data Mining (SDM '14)*. Society for Industrial and Applied Mathematics, Philadelphia, USA, 839–847. doi:10.1137/1.9781611973440.96
- [27] Niklas Muennighoff, Nouamane Tazi, Loïc Magne, and Nils Reimers. 2023. MTEB: Massive Text Embedding Benchmark. arXiv:2210.07316
- [28] Ben Nagy. 2015. *Crashwalk*. Retrieved Jan. 13, 2025 from <https://github.com/bnagy/crashwalk>
- [29] OpenAI. 2020. *OpenAI Python API Library*. Retrieved Jan. 13, 2025 from <https://github.com/openai/openai-python>
- [30] OpenAI. 2024. *New Embedding Models and API Updates*. Retrieved Jan. 13, 2025 from <https://openai.com/index/new-embedding-models-and-api-updates>
- [31] F. Pedregosa, G. Varoquaux, A. Gramfort, V. Michel, B. Thirion, O. Grisel, M. Blondel, P. Prettenhofer, R. Weiss, V. Dubourg, J. Vanderplas, A. Passos, D. Cournapeau, M. Brucher, M. Perrot, and E. Duchesnay. 2011. Scikit-Learn: Machine Learning in Python. *Journal of Machine Learning Research* 12 (2011), 2825–2830.
- [32] Van-Thuan Pham, Sakaar Khurana, Subhajit Roy, and Abhik Roychoudhury. 2017. Bucketing Failing Tests via Symbolic Analysis. In *2017 Fundamental Approaches to Software Engineering (FASE '17, Vol. 10202)*. Springer Berlin Heidelberg, Berlin, Heidelberg, 43–59. doi:10.1007/978-3-662-54494-5\_3
- [33] Nils Reimers and Iryna Gurevych. 2019. Sentence-BERT: Sentence Embeddings Using Siamese BERT-Networks. In *Proceedings of the 2019 Conference on Empirical Methods in Natural Language Processing and the 9th International Joint Conference on Natural Language Processing (EMNLP-IJCNLP '19)*. Association for Computational Linguistics, Hong Kong, China, 3980–3990. doi:10.18653/v1/D19-1410
- [34] Peter J. Rousseeuw. 1987. Silhouettes: A Graphical Aid to the Interpretation and Validation of Cluster Analysis. *J. Comput. Appl. Math.* 20 (Nov. 1987), 53–65. doi:10.1016/0377-0427(87)90125-7
- [35] The afl-utils developers. 2015. *Afl-Utils*. Retrieved Jan. 13, 2025 from <https://gitlab.com/rc0r/afl-utils>
- [36] The MITRE Corporation. 1999. CVE – Common Vulnerabilities and Exposures. Retrieved Jan. 13, 2025 from <https://www.cve.org/>
- [37] The MITRE Corporation. 2024. CWE – Common Weakness Enumeration. Retrieved Jan. 13, 2025 from <https://cwe.mitre.org/>
- [38] Rijnard Van Tonder, John Kotheimer, and Claire Le Goues. 2018. Semantic Crash Bucketing. In *Proceedings of the 2018 33rd ACM/IEEE International Conference on Automated Software Engineering (ASE '18)*. ACM, Montpellier, France, 612–622. doi:10.1145/3238147.3238200
- [39] Roman Vasiliev, Dmitriy Koznov, George Chernishev, Aleksandr Khvorov, Dmitry Luciv, and Nikita Povarov. 2020. TraceSim: A Method for Calculating Stack Trace Similarity. In *Proceedings of the 2020 4th ACM SIGSOFT International Workshop on Machine-Learning Techniques for Software-Quality Evaluation (MaTeSQuE 2020)*. ACM, Virtual, USA, 25–30. doi:10.1145/3416505.3423561
- [40] Michal Zalewski. 2013. *AFL: American Fuzzy Lop*. Retrieved Jan. 13, 2025 from <https://lcamtuf.coredump.cx/afl/>
- [41] Dun Zhang, Jiacheng Li, Ziyang Zeng, and Fulong Wang. 2025. Jasper and Stella: Distillation of SOTA Embedding Models. arXiv:2412.19048
- [42] Xing Zhang, Jiongyi Chen, Chao Feng, Ruilin Li, Wenrui Diao, Kehuan Zhang, Jing Lei, and Chaojing Tang. 2022. DeFault: Mutual Information-based Crash Triage for Massive Crashes. In *Proceedings of the 2022 44th International Conference on Software Engineering (ICSE '22)*. ACM, Pittsburgh, USA, 635–646. doi:10.1145/3510003.3512760